

Institute of Physics and Power Engineering, Obninsk, Russia

IVAN N. BORZOV, WIESŁAW A. KAMIŃSKI\*

*Selfconsistent Neutron Densities  
in Heavy Nuclei and Neutron Halo*

---

Samozgodne gęstości neutronów w ciężkich jądrach i halo neutronowe

1. INTRODUCTION

The periphery of the atomic nucleus has remained a puzzle up till now. Researches on the neutron halo shed a new light on this problem and renew an interest of both experimentalists and theorists [1–5]. Experimental discoveries suggest large differences in neutron densities in the light neutron-rich isotopes [6–8]. Also different distributions for neutron and proton matter are reported in the light and heavy nuclei [4, 9, 10]. All these phenomena require our much deeper understanding of the nuclear models. Simultaneously, the experimental data give us an unique opportunity to test these models in the region where they have not been yet applied seriously. In particular, one can look for density distributions of neutrons  $\rho_n(r)$  and protons  $\rho_p(r)$  at the large nuclear distance  $r$ .

There were a few models used for explanation of the difference between proton and neutron distributions in nuclei. The simple nuclear asymptotic density model originated from the idea of Bethe and Siemens [11]

---

\* Institute of Physics, M. Curie-Skłodowska University, 20-031 Lublin, pl. M. Curie-Skłodowskiej 1, Poland.

generates average level densities but lacks deformation and shell effects, as well as pairing correlations [4]. Another approach involving a self-consistent method is more reliable because it takes into account both the shell effects and pairing correlations. In some interpretations of the nuclear halo in heavy nuclei the relativistic mean field theory was also applied [5].

In the present studies we have used the self-consistent Fermi-system approach with pairing. Recently this method has been successfully applied in the beta decay of the neutron-deficient tin isotopes to describe the Gamov-Teller transitions [12]. It has been also used as a framework for description of the neutrino scattering [13]. Problems which were addressed in such researches are calculations of some nuclear observables like binding energies, separation energies of proton and neutron and mean-squared radii  $\langle r^2 \rangle$ . Rather satisfactory agreement of the experimental data gives hope for such a model to be sufficiently reliable to study the problem addressed in the present work.

## 2. NUCLEAR DENSITIES WITHIN FFS-THEORY

The general scheme of the approach includes construction of the self-consistent potential and generation of the quasiparticle basis. For proper description of the density distribution one needs to construct the mean fields for neutrons and protons with pairing correlations effects included. We employ the density functional method based on the quasiparticle Hamiltonian with the free kinetic energy operator, so that the effective mass of a quasiparticle is taken to be equal to the bare nucleon mass. A quasiparticle spectrum and wave functions are calculated with a self-consistent mean field which is the first variational derivative of the density functional. As the effective mass of a nucleon on the Fermi surface in atomic nuclei is close to its bare mass, one can hope that the calculated spectrum of quasiparticle levels will be close to the observed one. If it is so, we may expect satisfactory description of the ground state and low-lying collective states.

The framework used in this paper is, in fact, a version of the self-consistent FFS theory [14] which has much in common with the Hartree-Fock method with effective forces [15]. The main problem of its practical application is the form and parametrization of the appropriate density functional. Here we use the density functional in the form suggested in ref. 16, where a dependence on  $\rho$  is simulated by the simple fractional-linear functions and the surface contribution is related with the finite-range forces.

The interaction energy density is represented as

$$\varepsilon_{\text{int}} = \varepsilon_{\text{main}} + \varepsilon_{\text{Coul}} + \varepsilon_{\text{sl}} + \varepsilon_{\text{pair}} , \quad (1)$$

where

$$\varepsilon_{\text{main}} = \frac{2}{3} \epsilon_F^0 \rho_0 \left[ a_+^v x_+^2 f_+^v + a_-^v x_-^2 f_-^v + a_+^s x_+ f_+^s \widetilde{f_+^s x_+} + a_-^s x_- f_-^s \widetilde{f_-^s x_-} \right] . \quad (2)$$

In the above equation  $x_{\pm} = (\rho_n \pm \rho_p)/2\rho_0$ ,  $\rho_{n(p)}$  is the neutron (proton) density,  $\rho_0$  means the equilibrium nuclear matter density ( $N = Z$ ) and  $\epsilon_F^0$  is the nuclear matter Fermi energy. We also defined interaction constants as follows:

$$f_{\pm}^v = \frac{1 - h_{1\pm}^v x_{\pm}}{1 + h_{2\pm}^v x_{\pm}} , \quad f_{\pm}^s = \frac{1}{1 + h_{\pm}^s x_{\pm}} , \quad (3)$$

$$\widetilde{f_{\pm}^s x_{\pm}} = \int D(\vec{r} - \vec{r}') f_{\pm}^s(\vec{r}') x_{\pm}(\vec{r}') d\vec{r}' , \quad (4)$$

where

$$D(\vec{r} - \vec{r}') = \delta(\vec{r} - \vec{r}') - \frac{1}{4\pi R^2} \frac{1}{|\vec{r} - \vec{r}'|} \exp\left(\frac{-|\vec{r} - \vec{r}'|}{R}\right) . \quad (5)$$

In the momentum representation

$$D(q) = \frac{(qR)^2}{1 + (qR)^2} . \quad (6)$$

In this case the last two terms of eq. (2) corresponding to the surface isoscalar and isovector potential energies are generated by the density-dependent finite-range forces.

The energy density of the Coulomb interaction  $\varepsilon_{\text{Coul}}$  is taken in an usual form with the exchange part in the Slater approximation.

$$\varepsilon_{\text{Coul}} = 2\pi e^2 \rho_p(r) \left( \frac{1}{r} \int_0^r \rho_p(r) r^2 dr + \int_r^\infty \rho_p(r) r dr \right) - \frac{3}{4} \left( \frac{3}{\pi} \right)^{1/3} e^2 \rho_p^{4/3}(r) . \quad (7)$$

The spin-orbit term  $\varepsilon_{\text{sl}}$  comes from the spin-orbit  $(\kappa + \kappa' \vec{\tau}_1 \cdot \vec{\tau}_2)[\vec{\nabla}_1 \delta(\vec{r}_1 - \vec{r}_2) \times (\vec{p}_1 - \vec{p}_2)] \cdot (\vec{\sigma}_1 + \vec{\sigma}_2)$  and the velocity spin-dependent  $(g_1 + g_1' \vec{\tau}_1 \cdot \vec{\tau}_2)(\vec{\sigma}_1 \cdot \vec{\sigma}_2)(\vec{p}_1 \cdot \vec{p}_2)$  interactions. For spherical nuclei this term can be expressed through the spin-orbit densities

$$\rho_{\text{sl}}^{n(p)}(\vec{r}) = \sum_{\lambda} n_{\lambda} \langle \vec{\sigma} \cdot \vec{l} \rangle_{\lambda} |\varphi_{\lambda}^{n(p)}(\vec{r})|^2 , \quad (8)$$

where  $n_\lambda$  is an occupation number of the single-particle level  $\lambda$ ,  $\varphi_\lambda$  — the single-particle wave function,  $\lambda = nljm\tau$  means the standard set of single-particle quantum numbers, and  $\langle \vec{\sigma} \cdot \vec{l} \rangle_\lambda = j(j+1) - l(l+1) - 3/4$ . For the corresponding energy density one obtains

$$\varepsilon_{sl} = C_0 r_0^2 \sum_{i,k=n,p} \left( \frac{1}{r} \rho_{sl}^i \kappa^{ik} \frac{d\rho}{dr} + \frac{1}{4r^2} \rho_{sl}^i g_1^{ik} \rho_{sl}^k \right), \quad (9)$$

where  $\kappa^{nn} = \kappa^{pp} = \kappa + \kappa'$ ,  $\kappa^{np} = \kappa^{pn} = \kappa - \kappa'$ ;  $g_1^{nn} = g_1^{pp} = g_1 + g_1'$ ,  $g_1^{np} = g_1^{pn} = g_1 - g_1'$ ;  $C_0 = 2\varepsilon_F^0/3\rho_0$ ,  $r_0 = (3/8\pi\rho_0)^{1/3}$ .

The last term in eq. (2), the pairing energy density  $\varepsilon_{\text{pair}}$ , is chosen to be

$$\varepsilon_{\text{pair}} = \frac{1}{2} \nu \mathcal{V} \nu, \quad (10)$$

where  $\nu$  is the anomalous nucleon density and  $\mathcal{V}$  plays the role of effective force in the particle-particle channel. In this paper such a force is represented in the simplest form of  $\delta$ -force

$$\mathcal{V}^{nn} = \mathcal{V}^{pp} = C_0 f^\xi \delta(\vec{r} - \vec{r}'), \quad (11)$$

where  $f^\xi$  is a dimensionless interaction constant of the FFS theory [15]. The superscript  $\xi$  refers to the energy cut-off parameter which defines the number of single-particle levels taken into account when evaluating the anomalous Green's functions and, correspondingly, when solving equations for pairing fields  $\Delta(\vec{r})$  and chemical potentials  $\mu$ .

The total interaction energy of superfluid nucleus  $E_{\text{int}}[\rho, \nu] = \int d\vec{r} \varepsilon_{\text{int}}(\vec{r})$ , with  $\varepsilon_{\text{int}}(\vec{r})$  defined in eqs. (1)–(11) is a functional of the normal  $\rho(\vec{r})$  and the anomalous  $\nu(\vec{r})$  densities. Self-consistent calculations with such a functional look like the standard variational HFB procedure in which the single-particle Hamiltonian takes the form

$$\mathcal{H} = \begin{pmatrix} h - \mu & -\Delta \\ -\Delta & \mu - h \end{pmatrix}. \quad (12)$$

In this formula we involved the definitions:

$$h = \frac{p^2}{2m} + \frac{\delta E[\rho, \nu]}{\delta \rho}, \quad \Delta = -\frac{\delta E[\rho, \nu]}{\delta \nu}. \quad (13)$$

Eq. (12) can be solved iteratively: For the given densities ( $\rho^{(i)}, \nu^{(i)}$ ) functional (1) allows to generate the elements of the Hamiltonian  $\mathcal{H}$ , and what follows also its eigenvalues and wave functions ( $u^{(i)}, v^{(i)}$ ). The latter

can be used to calculate new densities ( $\rho^{(i+1)}, \nu^{(i+1)}$ ) which determine an input for the next iteration. This procedure is continued until complete convergency is achieved.

Parameters of the density functional (13) were chosen by fitting bound energies, charge distributions and single-particle spectra for magic nuclei  $^{40}\text{Ca}$ ,  $^{48}\text{Ca}$ ,  $^{208}\text{Pb}$  and for non-magic ones with both weak superfluidity ( $^{90}\text{Zr}$ ,  $^{146}\text{Gd}$ ) and developed pairing (even-even Sn and Pb isotopes). The pairing interaction was treated in diagonal approximation within all bound single-particle levels. To keep in the fitting procedure a number of parameters as low as possible one can assume that  $f_-^v = f_+^v$  (i.e.  $h_{1-}^v = h_{1+}^v$  and  $h_{2-}^v = h_{2+}^v$ ). Also the surface symmetry energy can be neglected ( $a_-^s = 0$ ). In such a case the following set of parameters is deduced:

$$\left. \begin{aligned} a_+^v &= -7.391, & h_{1+}^v &= 0.037, & h_{2+}^v &= 1.322, \\ & & a_-^v &= 3.595, \\ a_+^s &= 10.0, & h_{2+}^s &= 0.31, \\ & & \kappa^{pp} &= \kappa^{pn} = 0.205, \\ g_1^{pp} &= -g_1^{pn} = -0.11, \\ & & f^\xi &= -0.33, \\ R &= 0.35 \text{ fm}, & r_0 &= 1.135 \text{ fm}. \end{aligned} \right\} . \quad (14)$$

One can obtain the relations between these parameters and the nuclear matter characteristics:

$$\left. \begin{aligned} a_+^v &= \alpha + (5\alpha + 6)/5\eta, \\ h_{1+}^v &= 1 - \alpha/a_+^v \eta, \\ h_{2+}^v &= 1/\eta - 1, \\ a_-^v &= (3\beta^0/\epsilon_F^0 - 1)/f_-^v(x_+ = 1), \end{aligned} \right\} , \quad (15)$$

where

$$\alpha = 3\frac{\mu^0}{\epsilon_F^0} - \frac{9}{5}, \quad \eta = \frac{5K^0 + 6\epsilon_F^0}{18(\epsilon_F^0 - 5\mu^0)}. \quad (16)$$

The infinite nuclear matter parameter  $\mu^0$  is the chemical potential (binding energy per one nucleon),  $K^0$  means the incompressibility modulus.  $\epsilon_F^0$  and  $\beta^0$  are the Fermi energy and the symmetry energy, respectively. Values of the parameters used in the present work are:  $\mu^0 = -15.73$  MeV,  $K^0 = 135$  MeV,  $\epsilon_F^0 = 37.35$  MeV and  $\beta^0 = 31$  MeV.

An important part of calculations is an inclusion of the single particle continuum because of contribution of states far from the Fermi-surface to the propagators. It is a matter of basic importance that the radial part of the

Green functions used in the explicit form of the propagators are expressed in terms of regular and irregular solutions of the Schrödinger's equation for the single-particle continuum [17]. The pairing part of the propagators correctly describing transitions between the levels, for which the Fermi-surface smearing is essential can be calculated in a simple way [18]. Of course one can also use the single-particle levels near the Fermi surface fitted to the experimental data [19].

### 3. NEUTRON HALO IN HEAVY NUCLEI

The LEAR measurements [4] established large neutron halo factors for a number of heavier nuclei:  $^{58}\text{Ni}$ ,  $^{96}\text{Zr}$ ,  $^{96}\text{Ru}$ ,  $^{130}\text{Te}$ ,  $^{144}\text{Sm}$ ,  $^{154}\text{Sm}$ ,  $^{176}\text{Yb}$ ,  $^{232}\text{Th}$  and  $^{238}\text{U}$ . This result was described in the self-consistent Hartree-Fock and Hartree-Fock-Bogoliubov framework using the effective Skyrme force SkP [20]. Also a simple spherical relativistic mean field model was applied to discuss the experimental data [5]. It was shown that nuclear systems displaying well defined neutron halo behaviour are characterized by the large halo factor

$$f(r) = \frac{Z}{N} \log \left( \frac{\rho_n(r)}{\rho_p(r)} \right).$$

This means theoretical confirmation of the increase of the relative neutron density against the proton density in nuclear periphery for the above nuclei. Our calculations also confirm such a conclusion.

Figure 1 presents the neutron density against the nuclear distance for the nuclei under discussion. One can see large differences of the values in the peripheral part of the nuclei (4 fm  $\langle r \rangle$ ), which is even more dramatic for a very far nuclear distance (8 fm  $\langle r \rangle$ ). The latter influences the neutron halo factor (17) in a more pronounced way as can be deduced from Figure 2. The differences in densities of neutron and proton matter in the periphery of nucleus are of one order or more of magnitude. For almost all the nuclei under discussion the halo factors are promisingly large, so this nuclei are good candidates for the neutron halo systems. Only for  $^{144}\text{Sm}$  nucleus we have contrary behaviour which can be treated as a sign of the proton halo [5]. The main difference between the results presented in this paper and those reported in References 4 and 5 is the neutron halo factor for  $^{58}\text{Ni}$  nucleus which is a good candidate for the neutron halo system in our work.

It is worth noting that our model reproduces mean-square radii and the binding energies with the accuracy about 4% as can be seen from Table 1.

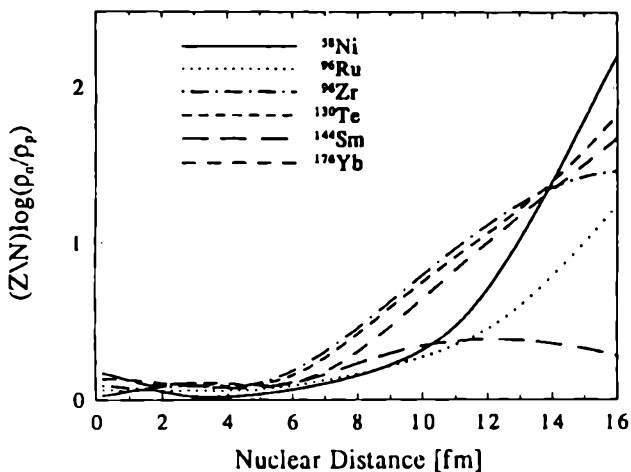


Fig. 1. The neutron density for  $^{58}\text{Ni}$  (solid line),  $^{96}\text{Ru}$  (dotted line),  $^{96}\text{Zr}$  (dashed-dotted line),  $^{130}\text{Te}$  (tiny-dashed line),  $^{144}\text{Sm}$  (long-dashed line),  $^{176}\text{Yb}$  (medium-dashed line). Wyznaczone gęstości neutronowe dla niklu  $^{58}\text{Ni}$  (linia ciągła), rutenu  $^{96}\text{Ru}$  (linia kropkowana), cyrkonu  $^{96}\text{Zr}$  (linia kreskowo-kropkowana), telluru  $^{130}\text{Te}$  (linia drobno kreskowana), samaru  $^{144}\text{Sm}$  (linia długo kreskowana) oraz iterbu (linia pośrednio kreskowana)

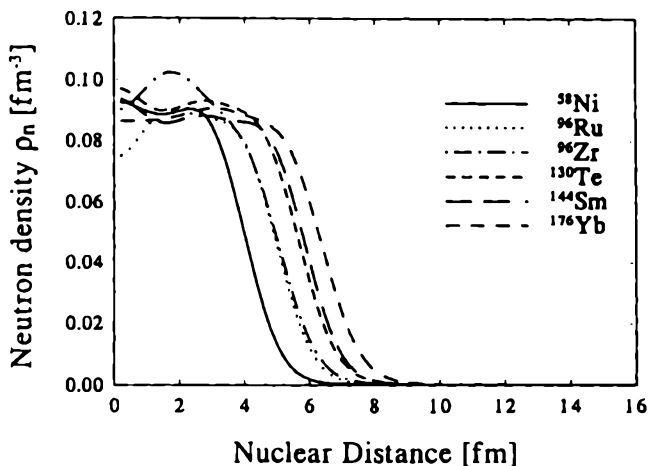


Fig. 2. The neutron halo factor as defined in eq. (17) for  $^{58}\text{Ni}$  (solid line),  $^{96}\text{Ru}$  (dotted line),  $^{96}\text{Zr}$  (dashed-dotted line),  $^{130}\text{Te}$  (tiny-dashed line),  $^{144}\text{Sm}$  (long-dashed line),  $^{176}\text{Yb}$  (medium-dashed line)

Czynnik halo [zdefiniowany rów. (17)] dla niklu (linia ciągła), rutenu (linia kropkowana), cyrkonu (linia kreskowo-kropkowana), telluru (linia drobno kreskowana), samaru (linia długo kreskowana), iterbu (linia pośrednio kreskowana)

In our opinion this result weakens the argument against the HF type models formulated in References 21.

A strong criticism of such a procedure results from the conviction that the method is unable to reproduce the proton and neutron separation energies as well as binding energies, which is not true from our calculations. A similar conclusion is formulated in Reference 4.

Tab. 1. The binding energies and mean-square radii calculated with the finite Fermi-system approach. The experimental data for the binding energies are from compilation 22. Data a and b are from refs. 23 and 24, respectively

Energie wiązania oraz średnie promienie kwadratowe wyznaczone metodą Fermiego dla systemu skończonego. Dane eksperymentalne zaczerpnięto z publikacji 22. Dane oznaczone (a) i (b) pochodzą odpowiednio z publikacji 23 i 24

Nucleus	$B_{\text{cal}}$	$B_{\text{exp}}$	$\sqrt{\langle r^2 \rangle_n}$	$\sqrt{\langle r^2 \rangle_p}$	$\sqrt{\langle r^2 \rangle_{\text{exp}}}$
$^{58}\text{Ni}$	500	506.454	3.6498	3.6470	3.77 <sup>a</sup>
$^{96}\text{Zr}$	824	828.994	4.3951	4.2156	4.40 <sup>a</sup>
$^{96}\text{Ru}$	821	826.490	4.3198	4.2787	—
$^{130}\text{Te}$	1091	1095.942	4.8448	4.6583	—
$^{144}\text{Sm}$	1190	1195.739	4.9562	4.8722	4.95 <sup>b</sup>
$^{176}\text{Yb}$	1400	1419.285	5.3775	5.1960	5.31 <sup>b</sup>

#### 4. CONCLUSIONS

In conclusion, the finite Fermi-system approach has been used to determine proton and neutron densities for a chain of heavy nuclei:  $^{58}\text{Ni}$ ,  $^{96}\text{Ru}$ ,  $^{96}\text{Zr}$ ,  $^{130}\text{Te}$ ,  $^{144}\text{Sm}$ ,  $^{176}\text{Yb}$ . Calculations were made within the self-consistent finite Fermi-system framework with pairing force. The calculated halo factors for these nuclei indicate a possibility of large differences between proton and neutron densities in the periphery of nuclei which makes the studies of such systems extremely interesting from both experimental and theoretical points of view. As predictions derived from different calculations provide some controversy about values of the neutron halo effects in concrete nuclei, further theoretical studies on this subject are necessary. Especially on

can expect researches which will shed more light on the role of specific effective interactions, especially pairing force in generating or attenuating of the neutron density excess. The problem of the nuclear deformation and its influence on the nuclear matter density in the periphery of nucleus must also be studied. Of course approximations connected with a choice of optical potential used in a description of antiproton densities can be simultaneously viewed. Some of these problems are of our interest and will be reported elsewhere.

#### ACKNOWLEDGMENTS

One of the authors (I.N.B.) is grateful to the colleagues from the Maria Curie-Skłodowska University in Lublin for the hospitality during his visits to the Theoretical Department of Physics. Valuable discussions with Dr A. Baran are acknowledged.

This work was supported in part by the State Committee for Scientific Researches (Poland) in the frame of Polish-German Agreement on collaboration in science and technology, decision No. C/2184/95.

#### REFERENCES

- [1] Tanihata I., Hamagaki H., Hashimoto O., Shida Y., Yoshikawa N., Sugimoto K., Yamakawa O., Kobayashi T. and Takahashi N., *Phys. Rev. Lett.*, 55 (1985) 2676.
- [2] Hansen P. G., Jonson B., *Europhys. Lett.*, 4 (1987) 409.
- [3] Hansen P. G., *Nucl. Phys. News*, 1 (1991) 21.
- [4] Lubański P., Jastrzębski J., Grochulska A., Stolarz A., Trzecińska A., Kurcewicz W., Hartmann F. J., Schmid W., von Egidy T., Skalski J., Smolańczuk R., Wycech S., Hilscher D., Polster D. and Rossner H., *Phys. Rev. Lett.*, 73 (1994) 3199.
- [5] Baran A., Pomorski K. and Warda M., to be published.
- [6] Bertulani C. A., Canto L. F. and Hussein M. S., *Phys. Rep.*, 226 (1993) 282.
- [7] Hansen P. G., *Nucl. Phys.*, A 553 (1993) 89c.
- [8] Zhukov M. V., Danilin B. V., Fedorov D. V., Bang J. M., Thompson and Vagan J. S., *Phys. Rep.*, 231 (1993) 151.
- [9] Jonson B. [in:] *Proceedings of the 5th International Conference on Nucleus-Nucleus Collisions*, Taormina 1994, *Nucl. Phys.*, A 574 (1994) 151c.
- [10] Batty C. J., Friedman E., Gils H. J. and Rebel H., *Adv. Nucl. Phys.*, 19 (1989) 1.
- [11] Bethe H. A., Siemens P. J., *Nucl. Phys.*, B 21 (1970) 589.
- [12] Borzov I. N., Fayans S. A., Krömer E. and Zawischa D., *Z. Physik*, A, to be published.
- [13] Borzov I. N., Trykov E. L. and Fayans S. A., *Nucl. Phys.*, A 564 (1995) 335.
- [14] Khodel V. A., Saperstein E. F., *Phys. Rep.*, 106 (1983) 111.
- [15] Migdal A. B., *Theory of Finite Fermi System and Atomic Nucleus Properties*, New York 1983.
- [16] Smirnov A. V., Tolokonnikov S. V. and Fayans S. A., *Sov. J. Nucl. Phys.*, 48 (1988) 1661.
- [17] Pyatov N. I., Fayans S. A., *Sov. J. Part. Nucl.*, 14 (1983) 953.

- [18] Borzov I. N., Trykov E. L., *Sov. J. Nucl. Phys.*, 52(1) (1990) 52; Borzov I. N., Trykov E. L. and Fayans S. A., *Sov. J. Nucl. Phys.*, 52 (1991).
- [19] Borzov I. N., Trykov E. L. and Fayans S. A., *Abstracts of WEIN-92 Dubna*, Dubna 1992, 39.
- [20] Dobaczewski J., Flocard H. and Treiner J., *Nucl. Phys.*, A 422 (1984) 103.
- [21] H. J. Körner H. J., Schiffer J. P., *Phys. Rev. Lett.*, 27 (1971) 1457.
- [22] Audi G., Wapstra A. H., *Nucl. Phys.*, A 565 (1993) 1.
- [23] Aufmuth P., Heilig K. and Steudel A., *Atom. Nucl. Dat. Tab.*, 37 (1987) 455.
- [24] Otten E. W., [in:] *Treatise on Heavy-Ion Science*, 8, New York 1989, 517.

### STRESZCZENIE

W niniejszym artykule wyznaczono gęstości materii neutronowej w kilku ciężkich jądrach (niklu, rutenu, cyrkonu, telluru, samaru i iterbu) używając metody Fermiego dla układów skończonych. Jakość rachunków typu samozgodnego, użytych przy generowaniu jądrowych funkcji falowych, została sprawdzona na przykładzie energii wiązania oraz średnich promieni kwadratowych. Pokazano możliwość wystąpienia w peryferyjnym obszarze nadmiarowej gęstości neutronów dyskutowanych jąder atomowych.